SUPPORTING INFORMATION: Conceptual uncertainties in groundwater and porewater fluxes estimated by radon and radium mass balances

S1. Radon and Radium data for the mass balance

S1.1. Surface water, porewater and stream water

Radon and radium data were collected concurrently in June 2016 (data previously published in Rodellas et al. (2018) and Tamborski et al. (2018)) (Fig. 1c and d). This data includes ^{222}Rn and ^{224}Ra concentrations in i) lagoon surface waters from the northern basin, which was sampled in discrete water samples for radium (n=40) and via continuous measurements of radon from a moving boat (n=59); ii) porewaters collected at 4 different locations (Pz1, Pz2, Pz3 and Pz4) and at different depths (from 5 to 50 cm below the sediment-water interface) using a direct-push, well-point piezometer (porewater profiles for Ra were collected in April 2016); and iii) discrete water samples from the permanent stream that flows into the lagoon and is fed by the main karstic groundwater spring (Fig. 1). Detailed methods for the collection and analyses of ^{222}Rn and ^{224}Ra in these samples are reported in Rodellas et al. (2018) and Tamborski et al. (2018), respectively. Note that the average ^{224}Ra concentration in lagoon water reported here is slightly different than that reported in Tamborski et al. (2018), because the southern lagoon was also included in the previous study.

Additional data was also collected to establish the short-term temporal variability of the short-lived tracers ^{222}Rn and ^{224}Ra in the lagoon. Lagoon ^{222}Rn concentrations were measured continuously at one site over 5 days (26 April – 1 May 2016) (Fig. 1a). Lagoon surface water was pumped continuously from the sampling station through a gas extraction membrane (Liqui-Cel MiniModule) which was coupled to a RAD7 detector, analyzing ^{222}Rn concentrations in hourly intervals (Dulaiova et al., 2005; Stieglitz et al., 2010; Schubert et al., 2012a). Water salinities and temperatures recorded continuously at the intake of the pump (CTD logger NKE S2T600) was used to correct the air-water partitioning of ^{222}Rn following (Schubert et al., 2012b). Further, eight ^{224}Ra surface water samples distributed throughout the northern basin were collected for ^{224}Ra analysis both on 22 June and 4 July 2017 (i.e. 12 days later). Radium

samples were filtered through MnO_2-coated acrylic fibers and analyzed using the RaDeCC system (Moore and Arnold, 1996).

All the data used in this study is available as Supporting Information (ResearchData).

S1.2. Sediment equilibration experiments

Porewater ^{222}Rn concentration in equilibrium with production from sediments was estimated by ^{222}Rn equilibration experiments using sediments from cores collected at 4 locations in the lagoon (Pz1, Pz2, Pz3, Pz4; Fig 1a),which were chosen to be representative of the different types of sediments in the lagoon as derived from a detailed sediment mapping (IFREMER, 2003). Subsequently, following (Chanyotha et al., 2014), , ~200 g of dry sediment was put into a 500 mL gas-tight reaction flask and the remaining volume was filled with Ra-free lagoon water. Each flask was connected in a closed loop to a RAD7 and the ^{222}Rn concentrations in overlying waters were continuously measured for 24 hours (1-hour cycles). ^{222}Rn diffusive fluxes were determined from the near-linear slope of ^{222}Rn concentration vs time.

S2. Estimation of porewater fluxes from ^{222}Rn deficit in sediments

The exchange of ^{222}Rn between overlying waters and sediments due to porewater fluxes and diffusion produces a deficiency of ^{222}Rn in sediments relative to the equilibrium porewater concentration, in which production from ^{226}Ra in sediments is balanced by radioactive decay. The integrated ^{222}Rn deficit over depth equals the total net flux of radon across the sediment-water interface and can be written as (Martin et al., 2007; Cable and Martin, 2008; Cook et al., 2018):

$$F_{sed} = \int_0^{\infty} \left(\lambda C_{eq-z} - \lambda C_z\right)\theta_z dz \qquad \text{(S1)}$$

where θ_z, $C_{eq\text{-}z}$ (Bq m^{-3}) and C_z (Bq m^{-3}) are sediment porosity, radon concentration in equilibrium with sediments and radon porewater concentration at each depth z (m). For simplicity, here we assume that θ_z and $C_{eq\text{-}z}$ are constant with depth, as often assumed in the literature (Cable and Martin, 2008; Cook et al., 2018). Constant θ is obtained from (Tamborski et al., 2018) and C_{eq} is derived from the maximum concentrations measured at each site (piezometers Pz1, Pz2 and Pz3). The ^{222}Rn concentrations measured in porewaters at different depths (C_z) at each location increase with depth (Fig. S1), indicating a deficit of C_z relative to C_{eq} for the upper sediments due to ^{222}Rn exchange between porewaters and overlying lagoon waters. The total net ^{222}Rn flux from sediments is estimated applying Eq. S1 and integrating the ^{222}Rn deficit down to the depth where the equilibrium concentration (C_{eq}) is reached. This total flux also includes the ^{222}Rn loss due to diffusion, which needs to be subtracted to obtain the ^{222}Rn flux that can mainly be attributed to advective porewater fluxes (Cook et al., 2018). In this case, we estimate ^{222}Rn diffusion by using the depth-independent approach (Equation 3), which is the only approach that provides an independent estimate by using the information derived from the porewater profiles (estimated C_{eq}). To upscale porewater fluxes derived from piezometers to the entire lagoon, we use an area-weighted average of porewater-driven ^{222}Rn fluxes by considering the distribution of sediments and assuming that recirculation fluxes at Pz4 (impermeable area) are negligible. Estimated porewater fluxes from this deficit model are 15 ± 3 Bq m^{-2} d^{-1}, which can be converted to a water

flow of 0.3 ± 0.1 cm d^{-1} (using the ^{222}Rn concentration measured at the shallowest point for each piezometer as the porewater endmember; (Cook et al., 2018)).

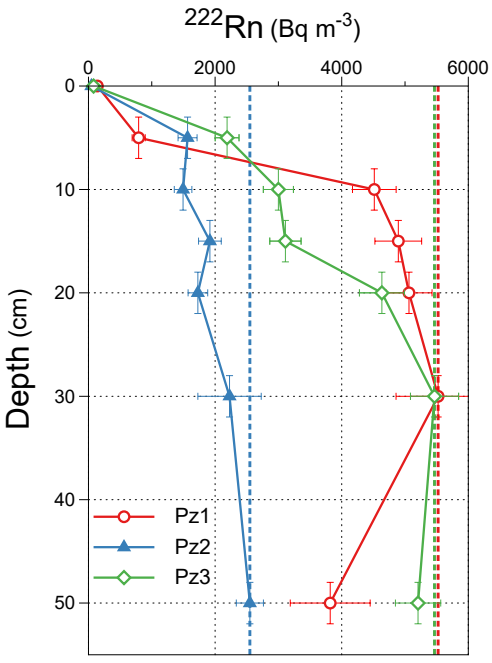

Figure S1: Depth profiles (in cm below the sediment-water interface) of ^{222}Rn concentration in porewater for the three piezometers collected in June 2016 (Rodellas et al., 2018). The dashed lines represent the assumed ^{222}Rn concentration in equilibrium with sediments (*i.e.* maximum observed porewater activities) and the solid areas represent the deficit of ^{222}Rn with respect to sediment equilibrium concentration.

REFERENCES

Cable J. E. and Martin J. B. (2008) In situ evaluation of nearshore marine and fresh pore water transport into Flamengo Bay, Brazil. *Estuar. Coast. Shelf Sci.* **76**, 473–483.

Chanyotha S., Kranrod C. and Burnett W. C. (2014) Assessing diffusive fluxes and pore water radon activities via a single automated experiment. *J. Radioanal. Nucl. Chem.* **301**, 581–588. Available at: http://link.springer.com/10.1007/s10967-014-3157-3 [Accessed April 5, 2019].

Cook P. G., Rodellas V., Andrisoa A. and Stieglitz T. C. (2018) Exchange across the sediment-water interface quantified from porewater radon profiles. *J. Hydrol.* **559**, 873–883.

Dulaiova H., Peterson R., Burnett W. C. and Lane-Smith D. (2005) A multi-detector continuous monitor for assessment of 222Rn in the coastal ocean. *J. Radioanal. Nucl. Chem.* **263**, 361–363. Available at: http://www.scopus.com/inward/record.url?eid=2-s2.0-17144397540&partnerID=tZOtx3y1 [Accessed January 30, 2014].

IFREMER (2003) *Réseau de Suivi Lagunaire du Languedoc-Roussillon: 4 - Etang de La Palme*., Sète, France.

Martin J. B., Cable J. E., Smith C., Roy M. and Cherrier J. (2007) Magnitudes of submarine groundwater discharge from marine and terrestrial sources: Indian River Lagoon, Florida. *Water Resour. Res.* **43**, n/a-n/a.

Moore W. S. and Arnold R. (1996) Measurement of223Ra and224Ra in coastal waters using a delayed coincidence counter. *J. Geophys. Res. C Ocean.* **101**, 1321–1329. Available at: http://www.scopus.com/inward/record.url?eid=2-s2.0-0029728946&partnerID=tZOtx3y1.

Rodellas V., Stieglitz T. C., Andrisoa A., Cook P. G., Raimbault P., Tamborski J. J., van Beek P. and Radakovitch O. (2018) Groundwater-driven nutrient inputs to coastal lagoons: The relevance of lagoon water recirculation as a conveyor of dissolved nutrients. *Sci. Total Environ.* **642**, 764–780.

Schubert M., Paschke A., Bednorz D., Bürkin W. and Stieglitz T. (2012a) Kinetics of the Water/Air Phase Transition of Radon and Its Implication on Detection of Radon-in-Water Concentrations: Practical Assessment of Different On-Site Radon Extraction

Methods. *Environ. Sci. Technol.* **46**, 8945–8951.

Schubert M., Paschke A., Lieberman E. and Burnett W. C. (2012b) Air-water partitioning of 222Rn and its dependence on water temperature and salinity. *Environ. Sci. Technol.* **46**, 3905–11. Available at: http://www.scopus.com/inward/record.url?eid=2-s2.0-84859348909&partnerID=tZOtx3y1 [Accessed January 30, 2014].

Stieglitz T. C., Cook P. G. and Burnett W. C. (2010) Inferring coastal processes from regional-scale mapping of 222Radon and salinity: examples from the Great Barrier Reef, Australia. *J. Environ. Radioact.* **101**, 544–52.

Tamborski J., Bejannin S., Garcia-Orellana J., Souhaut M., Charbonnier C., Anschutz P., Pujo-Pay M., Conan P., Crispi O., Monnin C., Stieglitz T., Rodellas V., Andrisoa A., Claude C. and van Beek P. (2018) A comparison between water circulation and terrestrially-driven dissolved silica fluxes to the Mediterranean Sea traced using radium isotopes. *Geochim. Cosmochim. Acta* **238**, 496–515.